Facile diazonium modification of pomegranate peel biochar: A stupendous derived relationship between thermal and Raman analyses

Ahmed M. Khalil[1,2,3,*], Radhia Msaadi[4], Wafa Sassi[4*], Imen Ghanmi[4], Rémy Pires[2], Laurent Michely[2], Youssef Snoussi[3], Alexandre Chevillot-Biraud[3], Stéphanie Lau-Truong[3], Mohamed M. Chehimi[2,3,*]

1 Photochemistry Department, National Research Centre, Dokki, Giza 12622, Egypt
2 Université Paris Est, CNRS, ICMPE (UMR 7182), 94320 Thiais, France
3 Université Paris Cité, CNRS, ITODYS (UMR 7086), 75013 Paris, France
4 Faculté des Sciences, Unité de Recherche Électrochimie, Matériaux et Environnement UREME (UR17ES45), Université de Gabès, 6000, Gabès, Tunisia

***** Correspondence : mohamed.chehimi@cnrs.fr ; mmchehimi@yahoo.fr (M.M.C.), wafa.sassi@issatgb.u-gabes.tn (WS); : akhalil75@yahoo.com (AMK).

Abstract:

There is an ever growing interest worldwide in the development of biochar from a large variety of agrowastes. This work contributes to the domain by tackling an agrowaste represented in pomegranate peels powder. The latter was activated by acid treatment and then pyrolyzed to generate low cost biochar. To enrich the surface of the resulting biochar, it was arylated with various *in-situ* generated diazonium salts of 4-aminobenzoic acid (H_2N-C_6H_4-COOH), sulfanilic acid (H_2N-C_6H_4-SO_3H) and Azure A dye. The effect of diazonium nature and concentration on the arylation process was monitored essentially using thermal gravimetric analysis (TGA), and Raman spectroscopy. These techniques showed gradual changes in the arylation of biochar at low concentrations of 10^{-5}, 10^{-4} and 10^{-3} M of 4-aminobenzoic acid. Interestingly, Azure A diazonium salt induces lower extent of surface modification, likely due to steric hindrance. One key feature of this work is the correlation between D/G Raman peak intensity ratio and the mass loading of the aryl groups. To the very best of our knowledge this is the first report ever on diazonium modification of agrowaste-derived biochar and opens new avenues for such carbon allotrope, *i.e.* surface arylation and applications.

Keywords: *Punica granatum*, agrowaste, diazonium salts, biochar, surface arylation.

Graphical Abstract

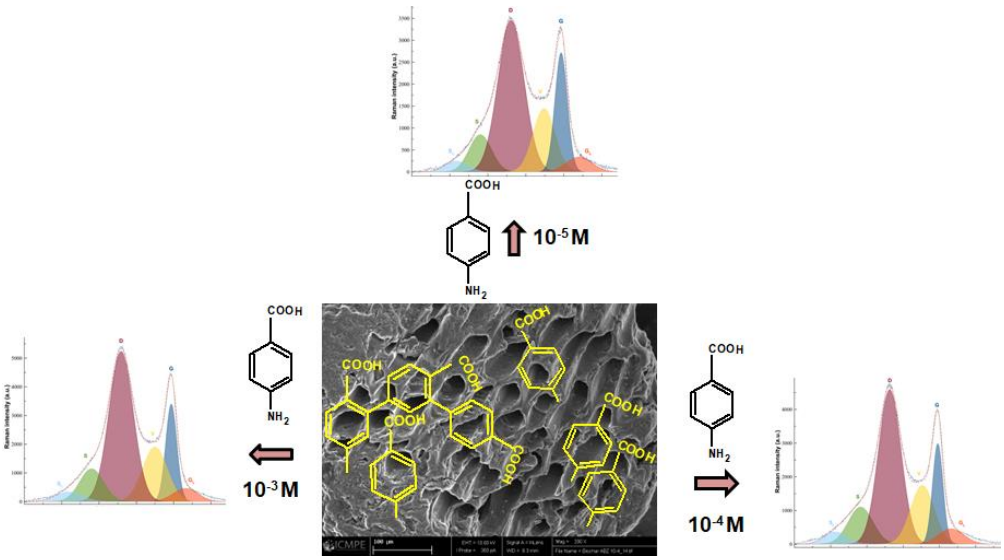

1. Introduction

Arylation of carbon allotropes is a very well established mean of preparing functional based carbon materials [1] for various applications comprising fillers [2] and reinforced polymeric matrices [3], support of (electro) nanocatalysts [4], flexible gas sensors [5, 6], electrode materials [7], and photovoltaic applications [8]. Although graphene, carbon nanotubes, fullerene are advanced carbon based materials [9], yet they are excessively expensive which limits the expansion of their utilization. Instead, one can take advantage of biochar(s) generated from the pyrolysis of agrowastes and other biomass resources[10, 11]. Biochar can be regarded as a promising candidate possessing several attractive features which can further be tuned via acid or base surface chemical treatment [12, 13], loading of alkali metal oxalate loading [14], amine functionalization using diethanolamine [15], or silanization [16]. However, arlyation with diazonium salts has much to offer due to the commercial availability of several aromatic amine precursors of diazonium compounds with several functional groups (-COOH, -NH_2, -SO_3H, perfluro alkyl chain, $N_3{\equiv}C$ azide, etc…) to control numerous physico-chemical properties and post reactivity [17].

Diazonium salts are chief surface modifiers and coupling agents as they spontaneously react with carbon allotropes [1, 17, 18]. This led us to reason that they could be employed to tailor the surface modification of biochar.

In this work, we bridge the best of two concepts: facile surface modification of carbon allotropes with diazonium salts and pyrolysis process to fabricate biochar from agrowaste (pomegranate peel powder). These materials derived from wastes have not been subjected to arylation using diazonium salts, hence the interest of this investigation. To the very best of our knowledge, no biochar designed by slow pyrolysis has been subjected to surface modification with aryl diazonium salts. On the scientific viewpoint we feature biochar modification in a facile way, at room temperature for multiple purposes. On the technological viewpoint, biochar have much to offer as functional materials when equipped with reactive aryl groups.

Subsequently, we describe the preparation procedure of biochar pyrolysis to pomegranate peels. These carbon allotropes were post functionalized with aryl diazonium salts comprising *in-situ* generated diazonium salts from 4- amino benzoic acid, sulfanilic acid and Azure A. Pristine and modified biochar materials were characterized by X-ray diffraction, scanning electron microscopy (SEM), X-ray photoelectron spectroscopy (XPS), thermal gravimetric analysis (TGA) and Raman spectroscopy.

2. Experimental

2.1. Chemicals

4-aminobenzoic acid, sulfanilic acid, $NaNO_2$ and HCl 37% were Aldrich products. Azure A was supplied by Alfa Aeser.

2.2. Biochar preparation

Pomegranate fruits were collected from the region of Kettana (Gabès region, Tunisia; Latitude: 33° 53' 17.0772" N, and Longitude: 10° 5' 51.0792" E). Biochar was prepared by pyrolysis of pomegranate peel dry powder. The peels were washed thoroughly until the washings were clear, and then dried in an oven at 100 °C for 24 h. The final dried peels were ground and pyrolyzed under nitrogen. 10 g of dried peel powder was heated with a temperature ramp of 10 °C/min; the final temperature was set at 1000 °C. The biochar was left then to cool down; the yield was about 21 %. The biochar was then acid-treated with H_3PO_4 (40 %) at 105 °C for 4 h.

2.3. Arylation of Biochar

200 mg of biochar were dispersed in 50 mL of deionized water under sonication for 10 min then kept in ice-water bath with maintaining the temperature in the range of 0-5 ^oC. For this dispersion, a 4-aminobenzoic acid solution was supplemented. The latter was prepared by dissolving a proper amount of 4-aminobenzoic in 5 mL of 37% HCl to have (10^{-3} M) concentration. The mixture was then maintained in an ice-water bath. An aqueous solution of $NaNO_2$ was then added with retaining the ratio of 1:1 between 4-aminobenzoic acid and $NaNO_2$. The reaction was pursued with stirring for 60 min. Thereafter, the suspension was centrifuged and washed several times with distilled water to remove any residues then dried.

The steps were repeated to synthesize arylated biochar-pomegranate with lower concentrations of aryl diazonium salt (10^{-4} M and 10^{-5} M) taking in consideration a fixed ratio of 1:1 between 4-aminobenzoic acid and $NaNO_2$.

The same arylation procedure to biochar was pursued by utilizing sulfanilic acid and Azure A as diazonium salts precursors at (10^{-3} M) instead of 4-aminobenzoic acid.

2.4. Characterization of biochar samples

An X'Pert-Pro Panalytical diffractometer was used to record diffraction pattern of the untreated biochar. A cobalt X-ray source (λ = 1.7889 Å) was used and the analysis was performed with Bragg-Brentano geometry.

Pristine and arylated biochar samples were characterized through Raman technique by using Horiba Labram HR Evolution machine fitted with a He−Ne laser beam the wavelength of which was set at 514 nm. The spectra were fitted using Magic Plot software, version 3.0.1.

TGA measurements were performed with a Setaram apparatus (Setsys Evolution model). The ramp was from RT to 800 °C at 10 °C/min heat rate under argon.

XPS analyses were conducted with a K Alpha+ machine (Thermo, East Grinstead, UK) fitted with a monochromated X-ray source (Al Kα, hν = 1486.6 eV) and a flood gun to compensate for the static charge build-up. To ensure detection of aryl group elemental markers, the pass energy was set at 80 eV for recording the narrow regions. Survey scans were acquired with pass energy of 200 eV. The powder samples were stuck on double-sided adhesive tapes. Data acquisition and processing was done using Avantage software, version 5.9902.

3. Results and Discussion

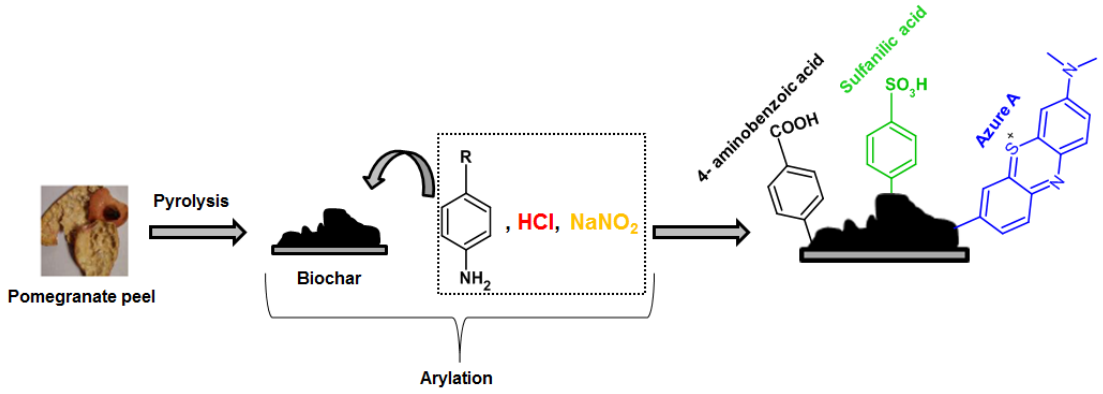

Figure 1. Schematic illustration of the preparation of arylated biochar from pomegranate peel agrowaste.

Figure 1 shows the pathway for the making of arylated biochar starting from pomegranate peel agrowaste. Characterization of arylated pomegranate-based biochar with different diazonium salts was done by monitoring different concentrations of 4-amino benzoic acid. We compared dizonium salts of 4-amino benzoic acid, sulfanilic acid and Azure A, at nominal concentration of 10^{-3} M. For benzoic acid, we have also tested 10^{-4} and 10^{-5} M initial concentrations. With its phenothiazine structure, Azure A could be considered as a bulky molecule compared to sulfanilic and 4-aminobenzoic acid. Blockage of the meta positions relative to the diazonium group (or the amino group in the precursor) rules out any possible

oligomerization of the phenothiazine moiety, as is the case of the 3,5-*bis*-tert-butyl benzenediazonium tetrafluoroborate.[19]

The XRD pattern of pomegranate based biochar is shown in Figure 2. Crystalline and semi-crystalline phases exist in biochar. Raising the pyrolytic temperature, boosts volatilizing the organic compounds.[20] Hence, it allows generating more pores. XRD pattern demonstrates the destruction of the crystalline structure. For this reason, relatively broad peaks appear at (2θ) = 24.6° and 44° [21, 22].

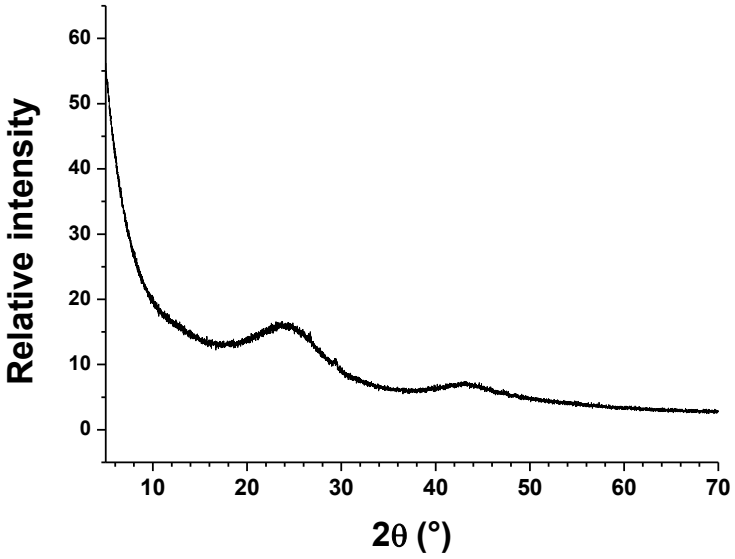

Figure 2. XRD of pomegranate peel biochar.

X-ray photoelectron spectra are displayed in Figure 3. All survey regions look practically the same; for the sake of clarity we display only the wide scan of the Biochar-Benzoic Acid 10^{-3} M (Figure 3a). S2p regions are displayed in Figures 3b-e; no sulfur is detected for the pristine biochar (Figure 3b) or Biochar-Benzoic Acid 10^{-3} M (Figure 3c). In contrast, arylation with sulfanilic acid yields an S2p centred at ~168 eV (Figure 3d) in line with a sulfonate chemical group,[23] whereas S2p from Biochar-Azure A is centred at ~164 eV due to the C-S-C environment of the sulfur atom in the attached dye[24] (see Figure 1). Conjugation of the C-S-C group within the hetrocyclic structure does not induce any significant shift toward higher binding energy position.

N1s peaks (not shown) were recorded for all samples and found to be quite noisy which is consistent with the quasi absence of N1s around 400 eV in the survey spectrum displayed in

Figure 3a. Biochar exhibits N1s due to persistent aminated groups from the initial biomass.[25, 26] For arylated samples, N1s regions could also arise from azo groups within the aryl layers,[27] but for Azure A, the dye contains *N*,*N*-dimethylamino group $-N(CH_3)_2$ group that contributes to the N1s region.

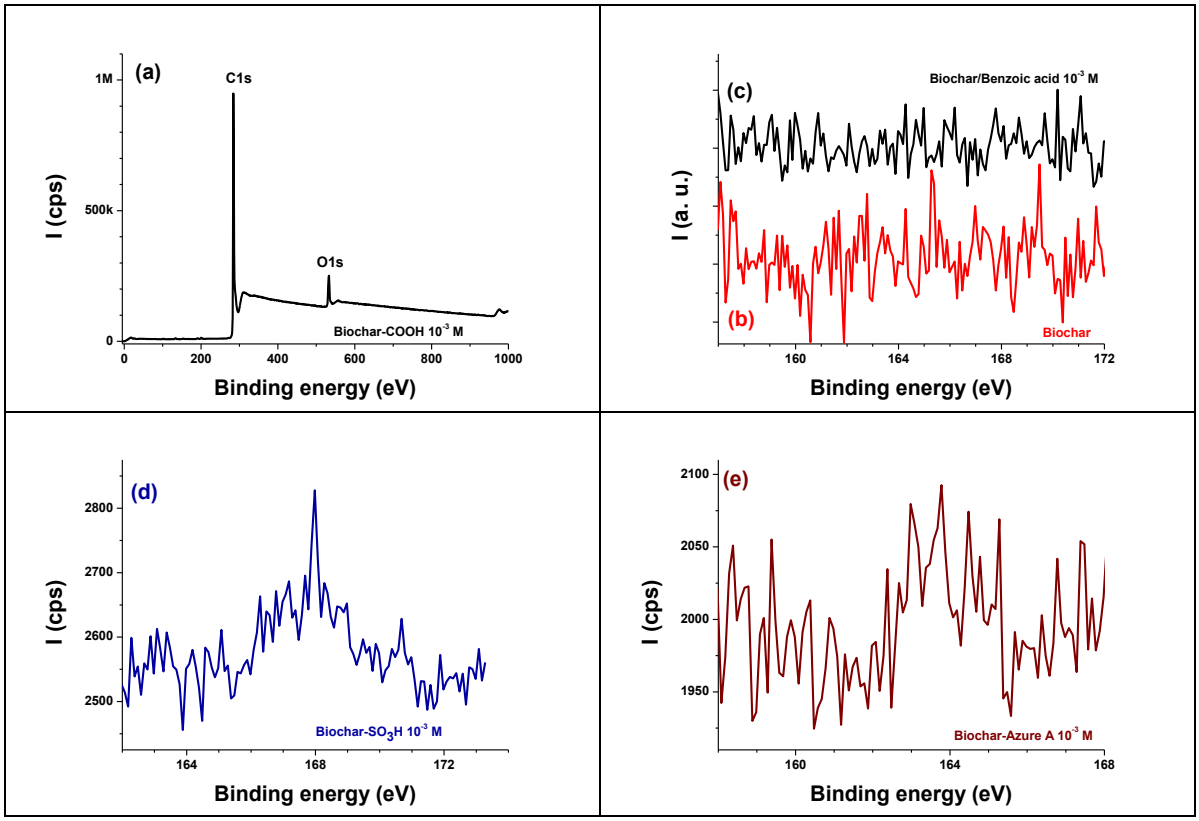

Figure 3. XP spectra from pristine and arylated biochar samples: (a) survey region of Biochar-Benzoic Acid 10^{-3} M, and S2p narrow regions of Biochar (b), Biochar-Benzoic Acid 10^{-3} M (c), Biochar-Sulfanilic acid 10^{-3} M (d), and Biochar-Azure A 10^{-3} M (e).

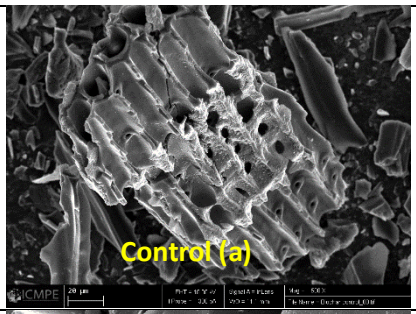
Control (a)

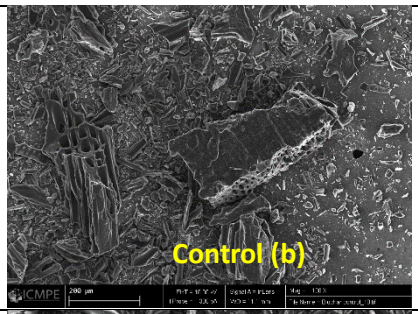
Control (b)

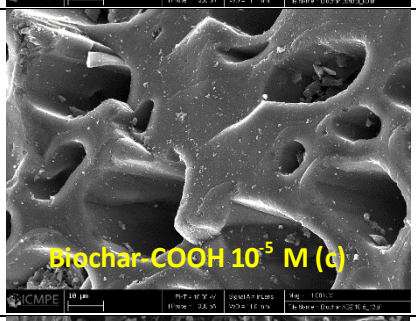
Biochar-COOH 10-5 M (c)


Biochar-COOH 10-5 M (d)

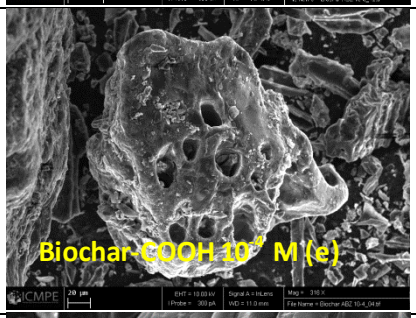
Biochar-COOH 10-4 M (e)

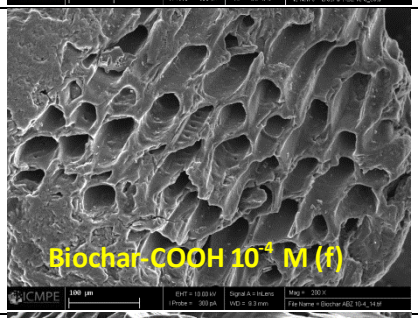
Biochar-COOH 10-4 M (f)

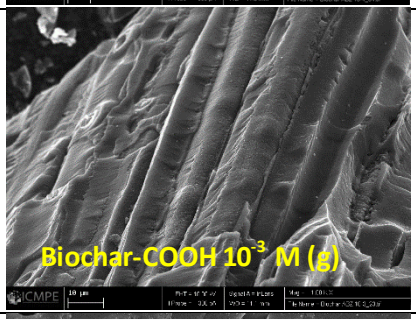
Biochar-COOH 10-3 M (g)

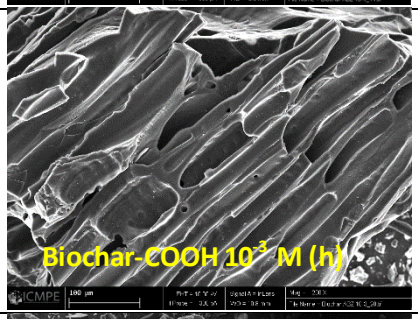
Biochar-COOH 10-3 M (h)

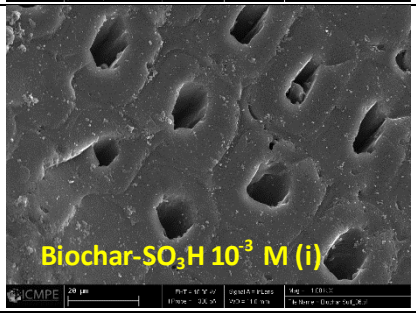
Biochar-SO3H 10-3 M (i)

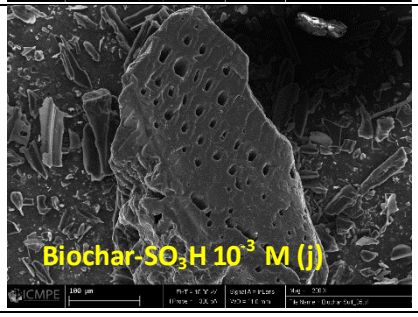
Biochar-SO3H 10-3 M (j)

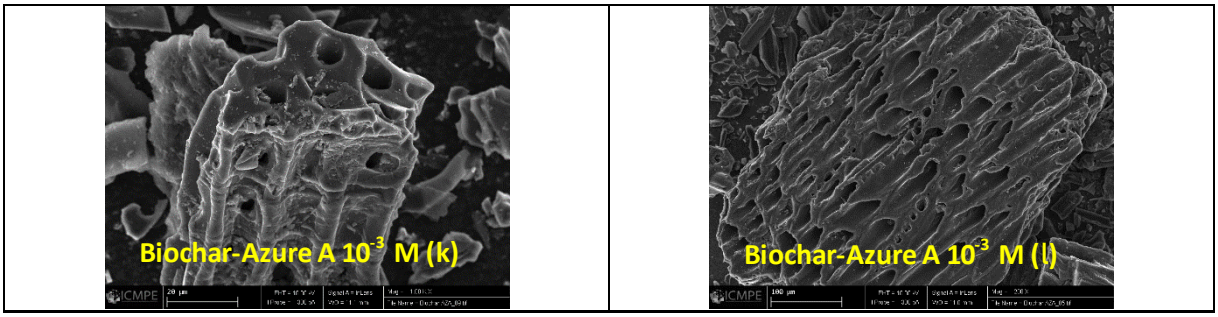

Figure 4. SEM images of unmodified and arylated biochar samples at low (b,d,f,h,j,l) and high magnification (a,c,e,g,i,k): control biochar (a,b), Biochar-COOH 10^{-5} M (c,d), Biochar-COOH 10^{-4} M (e,f), Biochar-COOH 10^{-3} M (g,h), Biochar-SO_3H 10^{-3} M (i,j), and Biochar-Azure A 10^{-3} M (k,l).

Figure 4 displays SEM images, at two magnifications, for the control and the modified biochar samples. Highly porous structures are noted due to the post-pyrolysis treatment of the biochar by phosphoric acid. Moreover, arylation has been performed with in situ-generated diazonium salts; that is in strong acid medium in the presence of the aromatic amines. Neither significant initial concentration effect is noted, nor the organic matter from the diazonium compounds blocks the biochar pores. Moreover, and despite arylation in harsh acidic media, the porous structure did not collapse.

Thermogravimetric analysis (TGA) was employed to investigate the thermal stability of the biochar upon being functionalized with various concentrations of aryl diazonium salts as shown in Figure 5a. The precursors of these salts are 4-aminobenzoic acid (10^{-5}, 10^{-4} and 10^{-3} M), sulfanilic acid and Azure A (10^{-3} M). The analysis was carried out in a temperature range up to 800 ^{o}C. The pyrolysis temperature has a role in determining the thermal stability of biochar. In Figure 5a, the control sample of pristine biochar showed a steady behavior upon increasing the temperature with maintaining its principal weight of biochar without considerable loss. The start of weight loss is monitored at 420 ^{o}C up to 747 ^{o}C. The functionalized samples of biochar exhibited a systematic behaviour in thermal stability as the sample showing the highest weight loss is for the functionalized one (10^{-3} M) 4-aminobenzoic acid. This is interesting to prove that as the concentration of aryl diazonium salt decreases in the sample, it approaches the thermal stability of pristine biochar sample. At relatively low temperature at 50 - 80 °C, the weight loss can be correlated to liberated adsorbed water. Some variations are observed at higher temperatures due to the degradation of functional groups on the surface of the samples. The samples with aryl diazonium salt show gradual weight loss

180 - 490 ^{o}C as a result of evolving volatiles. The weight loss in this stage may be ascribed to the decomposition as carbon turns to CO, CO_2 and CH_4. The lowest weight loss corresponds to biochar by losing 3 % of the original weight varying upon being functionalized by 4-aminobenzoic acid. Meanwhile, the highest concentration of the used diazonium salt precursor displays the highest weight loss to reach 14 % of its weight. As the concentration of the latter decreases, lower weight loss takes place approaching the control biochar sample. Above 490 ^{o}C, a faster weight loss takes place than the previous stage. Upon comparing the other diazonium salt precursors namely; sulfanilic acid and Azure A, one could notice a similar behaviour to the previously investigated samples as shown in Figure 3b. However, the sulfanilic acid-functionalized biochar shows higher thermal stability up to 584 ^{o}C, losing ~ 12 % of its original weight. On the other hand, the sample loaded with Azure A loses ~ 7 % at relatively lower temperature 503 ^{o}C.

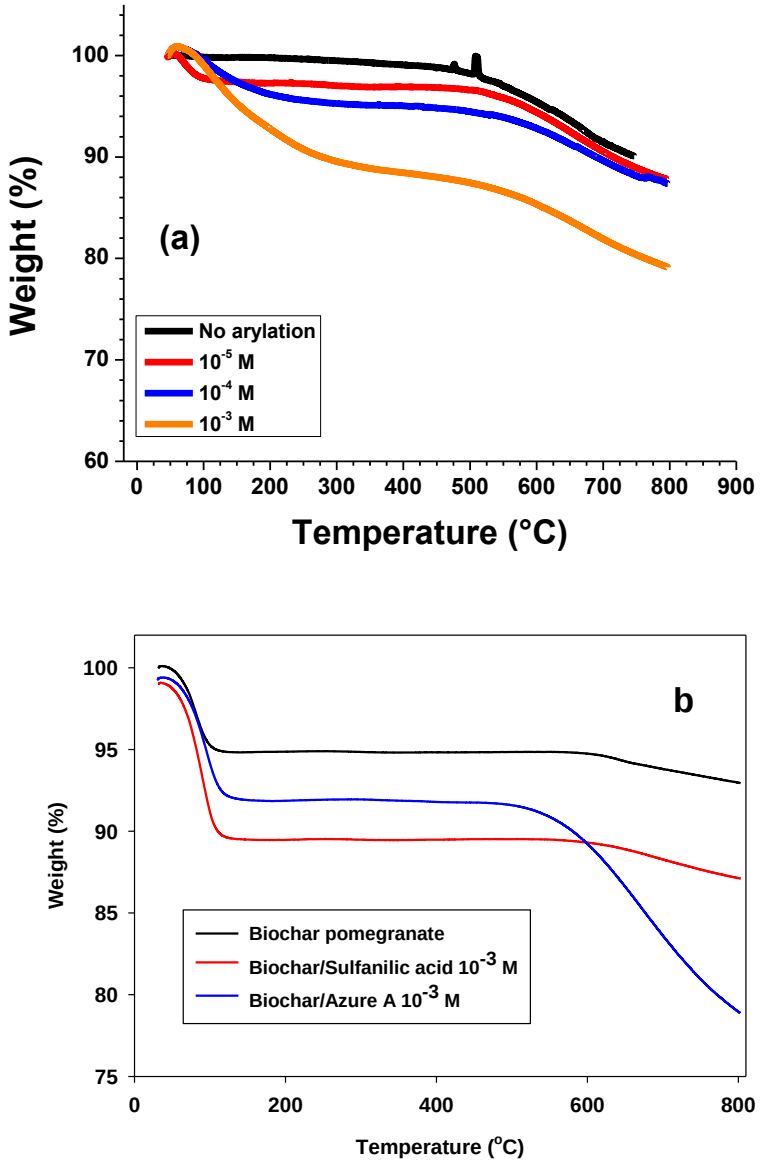

Figure 5. TGA thermograms of biochar loaded with: a) different concentrations of 4- aminobenzoic acid (10^{-3}, 10^{-4} and 10^{-5} M) b) sulfanilic aicd or Azure A (10^{-3} M).

3.3. Raman spectroscopy

Raman spectroscopy was used as a vibrational spectroscopy technique for determining the chemical functionalization and the dissemination of chemical bonds in the investigated biochar samples. Figure 6 displays peak-fitted Raman spectra of the tested biochar samples from 800 to 2000 cm^{-1}. The spectra were fitted with six main bands centered at 1080,1220, 1350, 1495, 1585 and 1690 cm^{-1}, assigned to S_L , S , D, V , G and G_L bands, respectively.[20, 28] The shoulder band, low (S_L) is most likely attributed to the circulation of hydrogen along

the biochar periphery.[28] The D band reflects the high regularization of the carbonaceous material with a combination of 6 or more benzene rings, and reveals a possible presence of heteroatoms and some defects.[20, 29]. The G band centered at 1585 cm^{-1}, and representing the graphitic region, reveals two kinds of vibrations, the quadrant one of the aromatic ring and the E2g 2 vibration of the biochar.[20] Centred at 1495 cm^{-1}, the V absorption band (the so-called valley V band) is ascribed to the mixture of two vibrational modes of sp^2 carbons, (i) the asymmetric stretch, and (ii) the breathing mode.[28] The D3 band between D and S_L bands is attributed to the sequence alkyl-alkyl ether.[20] The absorption band G_L illustrates the presence of carbonyl function in the biochar (C=O).[20] From Figure 6, one can clearly note substantial change in the D/G peak intensity ratio on going from the Biochar control sample (Figure 6a) to the most effective arylation, obtained for Biochar-COOH 10^{-3} M (Figure 6f). Clearly, arylation induces chemical modification which is very well probed by Raman spectroscopy;[30] this is despite the small changes noted using TGA in the actual case. The most important features D and G bands are also discussed in terms of nanometer-sized crystallites in the disordered structures , and the ordered graphite, respectively.[31]

The D/G peak height ratios vary through various samples of pristine or functionalized biochar as a result of biochar arylation.[32] In the literature, D/G peak height ratios are usually employed to track chemical modification of carbon. Herein, D/G peak height ratio increase with arylation regardless the nature of the diazonium compound compared to pristine biochar. However, taking advantage of the curve-fitting, one can instead consider the peak area of the D and G bands. Interestingly, Figures 6a,d-f show that the D/G relative peak area increases with the initial concentration of the 4-carboxybenzenediazonium salt. It is to note that lower concentrations for Biochar-SO_3H and Biochar-Azure A have not been tested due to the significantly small changes noted by TGA. Raman D/G peak intensity ratio has been related to the initial concentration of diazonium and iodonium salts used for arylation of carbon surface.[33]

From TGA and Raman analyses, we have derived a stupendous relationship between D/G peak area ratio versus the mass loading of aryl groups (in wt. %). The correlation rests on estimating the weight loss % of biochar(s) at 400 ^{o}C with respect to D/G ratio as shown in Figure 7a. It is important to note that D/G peak area ratio is related to the actual aryl mass loading and not to the initial concentration set for biochar modification. The plot shown in Figure 7a correlates two experimental results and this is not usually reported. Figure 7a displays a good correlation of D/G upon increasing the functionalization content with

diazonium salts onto biochar reaching a plateau region as a sign of saturation of these loadings on biochar surface. The increased mass loading for higher initial concentration of 4-carboxybenzenediazonium salt is due to the oligomerization of the aryl groups [17, 34]. Since, new aryl radicals attach to those already tethered to the biochar, clearly no further direct modification of biochar could be probed by Raman. This is the reason why at higher mass loading, a steady state D/G intensity ratio is reached for Biochar-COOH, in the same way it has been reported for 3,5-bis tertbutylbenzenediazonium compound on highly oriented pyrolytic graphite.[35] It is noteworthy that diazotized Azure A imparts the lowest modification of biochar, likely due to steric hindrance which prohibits oligomerization of Azure A units, given the blocked 3 and 4 positions of the aromatic ring attached to the surface. Similarly, anthraquinone-2-diazonium salt reaction with graphite surface yields aryl sub-monolayer due to the blockage of the 3 and 4 positions and the steric hindrance of the molecule;[36] this is the same situation for Azure A with its blocked meta position and steric hindrance. For this reason, there is less loading and thus low D/G peak area ratio. Elsewhere, it was demonstrated that on multiwalled carbon tubes, arylation with Azure A was found to yield the thinnest aryl layer compared to the diazonium salts of Neutral Red and Congo Red.[24] Yet, the pomegranate biochar modification with $–C_6H_4$-COOH groups at initial diazonium concentration of 10^{-5} M yields D/G = 2.67, higher than that of the pristine pomegranate biochar (D/G = 2.19). 10^{-3} M Azure A induces a D/G peak area ratio (2.38), even slightly lower than value comparable to that of Biochar-COOH 10^{-5} M (2.67), which shows that the band shape modification is not only concentration-dependent but is influenced by the nature of aromatic amine employed for arylation.

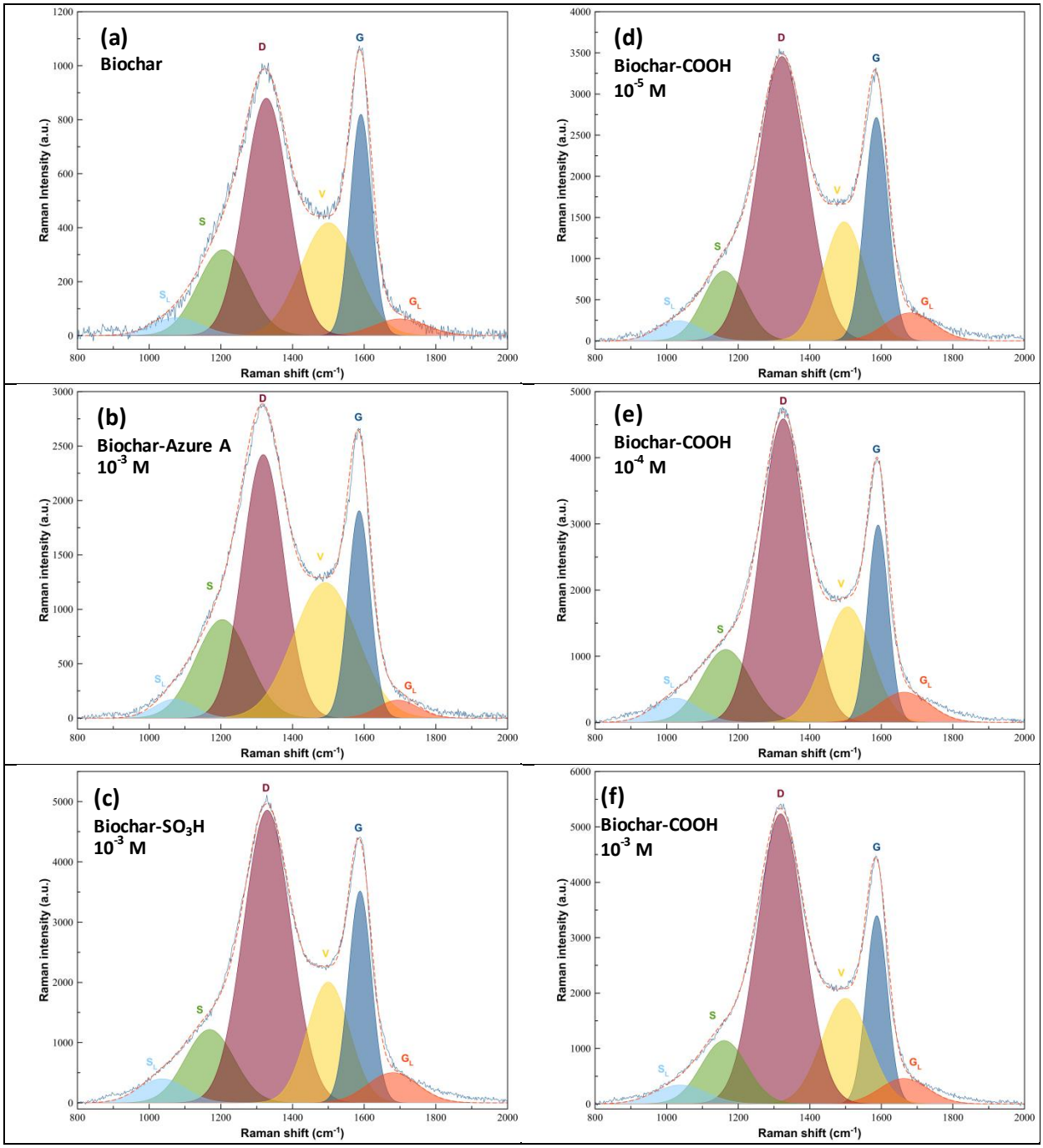

Figure 6. Peak-fitted Raman spectra of unmodified and arylated biochar: (a) control Biochar sample, (b) Biochar-Azure A 10^{-3} M, (c) Biochar-SO_3H 10^{-3} M, (d) Biochar-COOH 10^{-5}, (e) Biochar-COOH 10^{-4} M, and (f) Biochar-10^{-3} M.

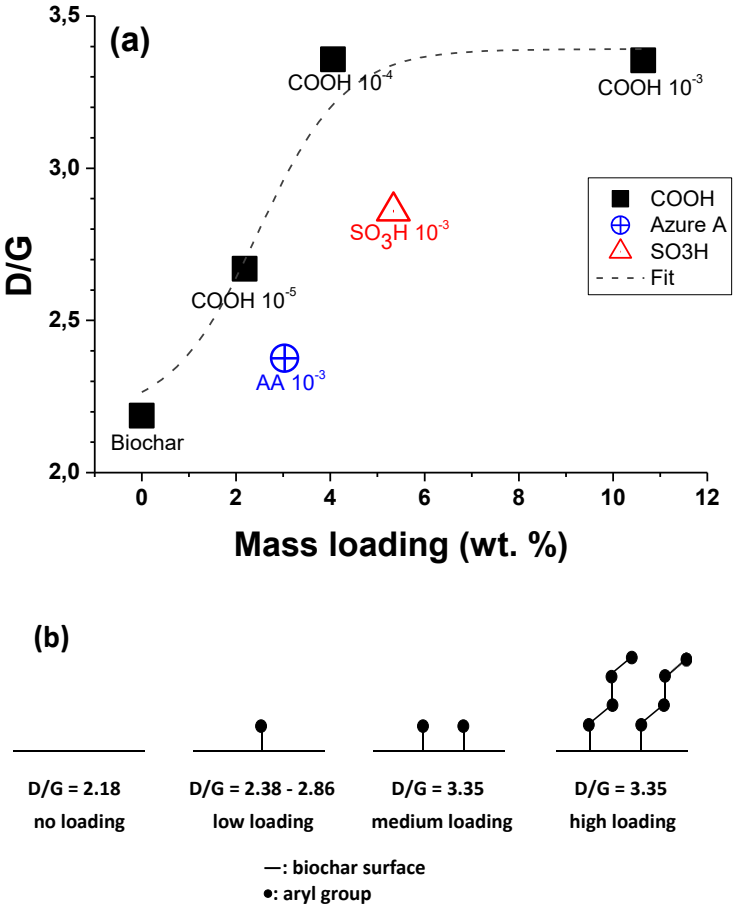

Figure 7. A relationship between D/G and mass loading (wt.%) for different biochar samples (a), and schematic illustration of stepwise aryl grafting density effect on D/G (b).

To account for the Raman-TGA results, Figure 7b schematically illustrates the effect of low, medium and high arylation of biochar on D/G peak intensity ratio. (Sub-)Monolayer deposition could be obtained for low initial concentration, followed by increased occupation of the surface and then oligomerization in the case of free meta-positions. High loading shown in Figure 7b is only possible for small and not for phenothiazine or anthraquinone-type aryl groups.

Conclusion

A biochar derived from pomegranate peel powder, as an agrowaste, has been prepared. The preparation step of biochar was carried out by pyrolysis at 1000 ^{o}C followed by functionalization through arylation with -COOH, -SO_3H and -$N(CH_3)_2$ diazonium salts. The diazo-precursors of these salts are 4- aminobenzoic acid, sulfanilic acid and Azure A. TGA analysis showed a proportional thermal stability of the investigated biochar samples with respect to the diazonium salts concentration. From the obtained TGA and Raman measurements, we have reached a striking relationship expressing the dependence of D/G ratio on the mass loading of biochar to reach a saturation condition at relatively high content of aryl-functionalization (using 10^{-3} M initial aromatic amine concentration). The steady state of D/G is likely to be due to oligomerization of aryl units. In this situation, there is no direct modification of biochar and thus no more increase in D/G value was noted. Interestingly, Azure A diazonium salt imparts lowest D/G value compared to other salts (at 10^{-3} M initial concentration) due to steric hindrance and thus limited arylation with bulky molecules.

To the very best of our knowledge, this is the first report on diazonium modification of biochar, prepared by slow pyrolysis of pomegranate peel. It interrogates both the effects of nature and concentration of diazonium compounds with possible or hindered oligomeration possibility. This first example could be adapted to any other agrowaste-derived biochar, which is another step towards the valorization of agrowastes.

Acknowledgements

A.M.K. and M.M.C. would like to thank both the French and Egyptian Governments for funding AMK's contribution through a fellowship granted by the French Embassy in Egypt (Institut Francais d'Egypte) and Science and Technology Development Fund (STDF)-Egypt, Project number (42248).

References

1. Gautier, C., Lopez, I., and Breton, T. (2021) A post-functionalization toolbox for diazonium (electro)-grafted surfaces: review of the coupling methods, *Materials Advances*.
2. Sandomierski, M., and Voelkel, A. (2020) Diazonium modification of inorganic and organic fillers for the design of robust composites: A review, *Journal of Inorganic and Organometallic Polymers and Materials*, 1-21.
3. Bensghaïer, A., Forro, K., Seydou, M., Lamouri, A., Mičušik, M., Omastová, M., Beji, M., and Chehimi, M. M. (2018) Dye diazonium-modified multiwalled carbon nanotubes: light harvesters for elastomeric optothermal actuators, *Vacuum 155*, 178-184.
4. Mirzaei, P., Bastide, S., Aghajani, A., Bourgon, J., Leroy, E., Zhang, J., Snoussi, Y., Bensghaier, A., Hamouma, O., and Chehimi, M. M. (2019) Bimetallic Cu–Rh Nanoparticles on Diazonium-

Modified Carbon Powders for the Electrocatalytic Reduction of Nitrates, *Langmuir 35*, 14428-14436.
5. Hamouma, O., Kaur, N., Oukil, D., Mahajan, A., and Chehimi, M. M. (2019) Paper strips coated with polypyrrole-wrapped carbon nanotube composites for chemi-resistive gas sensing, *Synthetic Metals 258*, 116223.
6. Guettiche, D., Mekki, A., Lilia, B., Fatma-Zohra, T., and Boudjellal, A. (2021) Flexible chemiresistive nitrogen oxide sensors based on a nanocomposite of polypyrrole-reduced graphene oxide-functionalized carboxybenzene diazonium salts, *Journal of Materials Science: Materials in Electronics 32*, 10662-10677.
7. Hetemi, D., Noël, V., and Pinson, J. (2020) Grafting of diazonium salts on surfaces: Application to biosensors, *Biosensors 10*, 4.
8. Lazzarin, L., Pasini, M., and Menna, E. (2021) Organic Functionalized Carbon Nanostructures for Solar Energy Conversion, *Molecules 26*, 5286.
9. Han, C., Li, Y.-H., Qi, M.-Y., Zhang, F., Tang, Z.-R., and Xu, Y.-J. (2020) Surface/Interface Engineering of Carbon-Based Materials for Constructing Multidimensional Functional Hybrids, *Solar Rrl 4*, 1900577.
10. Tripathi, M., Sahu, J. N., and Ganesan, P. (2016) Effect of process parameters on production of biochar from biomass waste through pyrolysis: A review, *Renewable and Sustainable Energy Reviews 55*, 467-481.
11. Harussani, M., and Sapuan, S. (2021) Development of Kenaf Biochar in Engineering and Agricultural Applications, *Chemistry Africa*, 1-17.
12. Zhang, D., Li, Y., Sun, A., Tong, S., Su, G., Jiang, X., Li, J., Han, W., Sun, X., and Wang, L. (2019) Enhanced nitrobenzene reduction by modified biochar supported sulfidated nano zerovalent iron: Comparison of surface modification methods, *Science of The Total Environment 694*, 133701.
13. Yang, C. X., Zhu, Q., Dong, W. P., Fan, Y. Q., and Wang, W. L. (2021) Preparation and characterization of phosphoric acid-modified biochar nanomaterials with highly efficient adsorption and photodegradation ability, *Langmuir 37*, 9253-9263.
14. Wang, L., and Shen, Y. (2021) Pyrolysis characteristics of cellulosic biomass in the presence of alkali and alkaline-earth-metal (AAEM) oxalates, *Cellulose 28*, 3473-3483.
15. Sajjadi, B., Chen, W.-Y., Mattern, D. L., Hammer, N., and Dorris, A. (2020) Low-temperature acoustic-based activation of biochar for enhanced removal of heavy metals, *Journal of Water Process Engineering 34*, 101166.
16. Sun, X., Qin, Y., Wu, B., Li, J., and Xue, C. (2019) Optimization of hydrophobic properties of biochar modified by silane coupling agent, *Environmental Science & Technology (China) 42*, 68-73.
17. Mohamed, A. A., Salmi, Z., Dahoumane, S. A., Mekki, A., Carbonnier, B., and Chehimi, M. M. (2015) Functionalization of nanomaterials with aryldiazonium salts, *Advances in colloid and interface science 225*, 16-36.
18. Mediavilla, M., Martínez-Periñán, E., Bravo, I., García-Mendiola, T., Revenga-Parra, M., Pariente, F., and Lorenzo, E. (2018) Electrochemically driven phenothiazine modification of carbon nanodots, *Nano Research 11*, 6405-6416.
19. Combellas, C., Kanoufi, F., Pinson, J., and Podvorica, F. I. (2008) Sterically Hindered Diazonium Salts for the Grafting of a Monolayer on Metals, *Journal of the American Chemical Society 130*, 8576-8577.
20. Cao, B., Yuan, J., Jiang, D., Wang, S., Barati, B., Hu, Y., Yuan, C., Gong, X., and Wang, Q. (2021) Seaweed-derived biochar with multiple active sites as a heterogeneous catalyst for converting macroalgae into acid-free biooil containing abundant ester and sugar substances, *Fuel 285*, 119164.
21. Zhang, T., Li, P., Fang, C., Jiang, R. F., Wu, S. B., and Nie, H. Y. (2013) Ammonium Nitrogen Removal from Wastewater by Biochar Adsorption, *Advanced Materials Research 726-731*, 1679-1682.

22. Xiao, G., Xiao, R., Jin, B., Zuo, W., Liu, J., and Grace, J. R. (2010) Study on electrical resistivity of rice straw charcoal, *Journal of Biobased Materials and Bioenergy 4*, 426-429.
23. Yoshihara, R., Wu, D., Phua, Y. K., Nagashima, A., Choi, E., Jayawickrama, S. M., Ishikawa, S., Liu, X., Inoue, G., and Fujigaya, T. (2022) Ionomer-free electrocatalyst using acid-grafted carbon black as a proton-conductive support, *Journal of Power Sources 529*, 231192.
24. Bensghaïer, A., Lau Truong, S. p., Seydou, M., Lamouri, A., Leroy, E., Mičušik, M., Forro, K., Beji, M., Pinson, J., and Omastová, M. r. (2017) Efficient covalent modification of multiwalled carbon nanotubes with diazotized dyes in water at room temperature, *Langmuir 33*, 6677-6690.
25. Yang, G., Chen, H., Qin, H., and Feng, Y. (2014) Amination of activated carbon for enhancing phenol adsorption: Effect of nitrogen-containing functional groups, *Applied Surface Science 293*, 299-305.
26. Yin, W., Guo, Z., Zhao, C., and Xu, J. (2019) Removal of Cr(VI) from aqueous media by biochar derived from mixture biomass precursors of Acorus calamus Linn. and feather waste, *Journal of Analytical and Applied Pyrolysis 140*, 86-92.
27. Buck, E., Lee, S., Stone, L. S., and Cerruti, M. (2021) Protein Adsorption on Surfaces Functionalized with COOH Groups Promotes Anti-inflammatory Macrophage Responses, *ACS Applied Materials & Interfaces 13*, 7021-7036.
28. Smith, M. W., Dallmeyer, I., Johnson, T. J., Brauer, C. S., McEwen, J.-S., Espinal, J. F., and Garcia-Perez, M. (2016) Structural analysis of char by Raman spectroscopy: Improving band assignments through computational calculations from first principles, *Carbon 100*, 678-692.
29. Li, C.-Z. (2007) Some recent advances in the understanding of the pyrolysis and gasification behaviour of Victorian brown coal, *Fuel 86*, 1664-1683.
30. Torréns, M., Ortiz, M., Turner, A. P., Beni, V., and O'Sullivan, C. K. (2015) Controlled Zn-Mediated Grafting of Thin Layers of Bipodal Diazonium Salt on Gold and Carbon Substrates, *Chemistry–A European Journal 21*, 671-681.
31. Ebner, E., Burow, D., Panke, J., Börger, A., Feldhoff, A., Atanassova, P., Valenciano, J., Wark, M., and Rühl, E. (2013) Carbon blacks for lead-acid batteries in micro-hybrid applications – Studied by transmission electron microscopy and Raman spectroscopy, *Journal of Power Sources 222*, 554-560.
32. Sampathkumar, K., Diez-Cabanes, V., Kovaricek, P., del Corro, E., Bouša, M., Hošek, J., Kalbac, M., and Frank, O. (2019) On the Suitability of Raman Spectroscopy to Monitor the Degree of Graphene Functionalization by Diazonium Salts, *The Journal of Physical Chemistry C 123*, 22397-22402.
33. Steeno, R., Rodríguez González, M. C., Eyley, S., Thielemans, W., Mali, K. S., and De Feyter, S. (2020) Covalent Functionalization of Carbon Surfaces: Diaryliodonium versus Aryldiazonium Chemistry, *Chemistry of Materials 32*, 5246-5255.
34. Belanger, D., and Pinson, J. (2011) Electrografting: a powerful method for surface modification, *Chemical Society Reviews 40*, 3995-4048.
35. Greenwood, J., Phan, T. H., Fujita, Y., Li, Z., Ivasenko, O., Vanderlinden, W., Van Gorp, H., Frederickx, W., Lu, G., Tahara, K., Tobe, Y., Uji-i, H., Mertens, S. F. L., and De Feyter, S. (2015) Covalent Modification of Graphene and Graphite Using Diazonium Chemistry: Tunable Grafting and Nanomanipulation, *ACS Nano 9*, 5520-5535.
36. Li, Q., Batchelor-McAuley, C., Lawrence, N. S., Hartshorne, R. S., and Compton, R. G. (2011) The synthesis and characterisation of controlled thin sub-monolayer films of 2-anthraquinonyl groups on graphite surfaces, *New Journal of Chemistry 35*, 2462-2470.